

Neural Architecture Ranker

Bicheng Guo¹, Shibo He¹, Tao Chen², Jiming Chen¹, Peng Ye²

¹Zhejiang University, ²Fudan University

{guobc, s18he, cjm}@zju.edu.cn

{eetchen, yepeng20}@fudan.edu.cn

Abstract

Architecture ranking has recently been advocated to design an efficient and effective performance predictor for Neural Architecture Search (NAS). The previous contrastive method solves the ranking problem by comparing pairs of architectures and predicting their relative performance, which may suffer generalization issues due to local pairwise comparison. Inspired by the quality stratification phenomenon in the search space, we propose a predictor, namely Neural Architecture Ranker (NAR), from a new and global perspective by exploiting the quality distribution of the whole search space. The NAR learns the similar characteristics of the same quality tier (i.e., level) and distinguishes among different individuals by first matching architectures with the representation of tiers, and then classifying and scoring them. It can capture the features of different quality tiers and thus generalize its ranking ability to the entire search space. Besides, distributions of different quality tiers are also beneficial to guide the sampling procedure, which is free of training a search algorithm and thus simplifies the NAS pipeline. The proposed NAR achieves better performance than the state-of-the-art methods on two widely accepted datasets. On NAS-Bench-101, it finds the architectures with top 0.01% performance among the search space and stably focuses on the top architectures. On NAS-Bench-201, it identifies the optimal architectures on CIFAR-10, CIFAR-100, and ImageNet-16-120. We expand and release these two datasets covering detailed cell computational information to boost the study of NAS.

1. Introduction

Deep neural networks (DNNs) have received great attention in recent years. Many DNNs that are artificially designed by researchers have been applied to many scenarios, such as image classification [15, 31], object detection [29, 30], semantic segmentation [3, 22] and other real-world applications [14, 42, 43]. Though these artificially designed DNNs have been proved to be powerful, designing

them requires rich human expertise and is labor-intensive. Furthermore, dedicated knowledge is needed in the network architecture design for many specific target domains.

Neural architecture search (NAS) offers a powerful tool for automating effective DNN designing for specific objectives. Previous studies directly apply different search and optimization methods, including Reinforcement Learning (RL) [26, 44], Evolutionary Algorithm (EA) [20, 27], and differentiable methods [2, 21], to find candidates in the search space. To reduce the prohibitive cost in evaluating a population of candidates, performance predictor is proposed to replace the evaluation metrics with the predicted performance of architectures [1, 25, 35]. However, these predictors try to approximate the absolute performance of the architecture and suffer the ranking problem [37], *i.e.*, the architectures with similar ground-truth performance have the incorrect predicted rankings due to the prediction bias. As a result, it misleads the search algorithm to select the low-ranking architectures and yields the deteriorate results.

The most recent contrastive method solves the ranking problem by comparing pairs of sampled architectures and calculating the probability that one architecture is better than the other [4]. Such an approach may suffer generalization issue because it only focuses on the rankings between two involved architectures and neglects the overall quality tiers¹ in the search space. Inspired by the architecture clustering phenomenon [38], we propose to learn and utilize these quality tiers: match each sampled architecture with the representation of different tiers, classify the architecture to the tier they belong and score it with the relative metric. Different from previous studies which locally learn the relative relationship between pair-wise architectures, we provide a new and global perspective to train the predictor by leveraging the architectures in various quality tiers. As a result, we are able to fully understand the quality distributions of the whole search space to improve the efficiency of the performance evaluation.

During the searching phase, most of the studies adopt

¹The definition of quality tier is that architectures are classified into multiple quality levels according to their ground-truth performance.

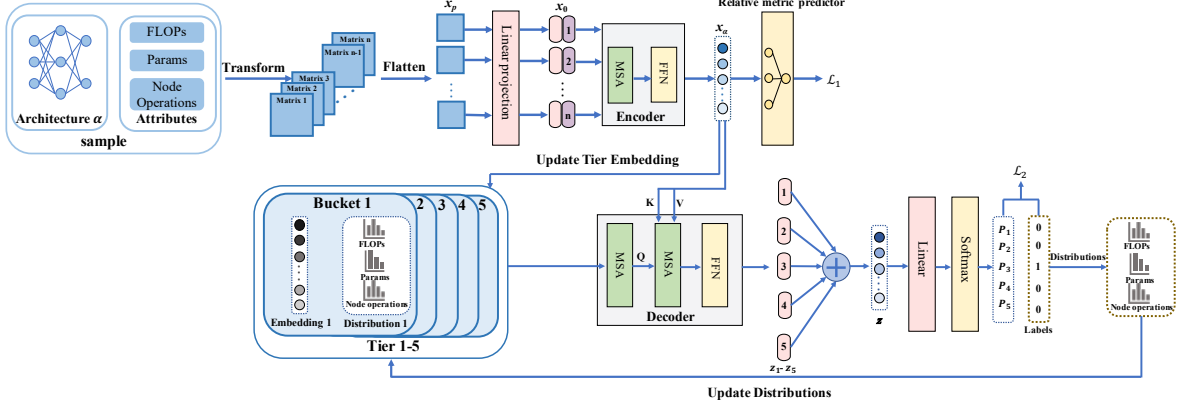


Figure 1. The overall training pipeline of the NAR. The NAR consists of encoder and decoder. The encoder extracts the feature of the sampled architecture and predicts its relative metric. The decoder matches the extracted feature with each of the tier embeddings and classifies it to the quality tier. The extracted features and batch distributions are updated to the corresponding tier according to the ground-truth performance of architectures.

reinforcement learning [32, 44] or evolutionary algorithms [13, 24], which requires additional training cost and complicates the NAS pipeline. Interestingly, we can benefit from collecting the distributions of top quality tiers and focus on the outperformed architectures by sampling with them in the search space. This makes our method free of training an RL controller or employing EA methods.

In this work, we propose a Neural Architecture Ranker (NAR) framework to learn the difference of various quality architectures in the search space and provide an accurate ranking for them. Firstly, the architectures in the training set are divided into five quality tiers and each is encoded to represent its structural and computational feature. Then, we match each sampled architecture with the embeddings of all tiers alternately to decide which quality tier it belongs to. In this way we relax the performance prediction into quality classification problem. We also leverage the extracted feature to predict the relative scores of the sampled architectures. Consequently, the NAR is capable of ranking and scoring the candidates according to their ground-truth performance in the search space. Furthermore, the distributions of the different quality tiers are collected to guide the sampling procedure in the searching phase, which requires no additional searching cost and simplifies the NAS pipeline. The overall contribution can be summarized as follows:

- Different from locally comparing pairs of architectures and calculating relative probability, we propose a Neural Architecture Ranker (NAR) that ranks and scores the architectures by matching them with the representation of various quality tiers from a global perspective.
- We propose to collect the distributions with different quality tiers to guide the sampling in the searching phase, which reduces cost in training an RL controller

or employing EA method like before.

- We achieve state-of-the art results on two widely accepted cell-based NAS datasets. On the NAS-Bench-101, our NAR with proposed sampling method finds the architecture with top 0.01% performance among the search space of 423k individual architectures. On the NAS-Bench-201, the proposed method finds the optimal architectures trained on CIFAR-10, CIFAR-100 and ImageNet-16-120.

2. Related Work

2.1. Neural architecture search

NAS offers to automate the design procedure of an efficient neural network given scenario constraints. It is often formulated as a constrained optimization problem:

$$\begin{aligned} & \min_{\alpha \in \mathcal{A}} \mathcal{L}(W_\alpha^*; \mathcal{D}_{val}), \\ & \text{s.t. } W_\alpha^* = \arg \min_{W_\alpha} \mathcal{L}(W_\alpha; \mathcal{D}_{trn}), \\ & \quad \text{cost}(\alpha) < \tau, \end{aligned} \quad (1)$$

where W_α are the weights of the architecture α , \mathcal{A} denotes the search space, \mathcal{D}_{trn} and \mathcal{D}_{val} mean the training and validation set respectively, $\mathcal{L}(\cdot)$ is the loss function, and $\text{cost}(\alpha)$ denotes the computational cost with respect to α , e.g. FLOPs, #parameters or latency for different devices. Pioneering work applies RL [16, 26, 32, 44] and EA [20, 27, 28] to select α to evolve into the training and validation procedure which endures prohibitive cost.

In order to save the evaluation cost and simplify the optimization difficulties, two-stage NAS decouples the training and searching into two separate steps [6, 13]. The first step

is to jointly optimize all the candidates in one supernet:

$$\min_W \mathbb{E}_{\alpha \in \mathcal{A}} [\mathcal{L}(W_\alpha; \mathcal{D}_{trn})]. \quad (2)$$

Then, RL or EA methods are utilized to select the subnet with best performance from the supernet given the constraints during the second searching phase:

$$\begin{aligned} \{\alpha_i^*\} &= \arg \min_{\alpha_i \in \mathbf{A}} \mathcal{L}(W_{\alpha_i}^*; \mathcal{D}_{val}) \\ \text{s.t. } \text{cost}(\alpha_i) &< \tau_i, \forall i, \end{aligned} \quad (3)$$

where W^* denotes the sharing weights inheriting from the trained supernet yielded in Eq. (1).

Quite a lot of attention has been paid to improve the training quality and efficiency of the supernet in Eq. (1), e.g., progressive shrinking [1], sandwich rule [39], attentive sampling [34] and ranking regulation [40]. During the searching phase, all of existing methods either train an RL controller, or employ the EA to select the candidates with top quality. In this paper, we try to avoid the cost of searching phase by collecting the distribution of outperformed architectures in the process of training the predictor and sampling according to them directly in the searching phase.

2.2. Predictor and the Ranking problem

To further boost the training and searching efficiency, the performance predictor is widely accepted both in one-stage and two-stage NAS [19]. FBNetV3 [7] applies a multi-layer perceptron to predict the accuracy and corresponding training recipe simultaneously. When training the supernet, predictor is utilized to facilitate the Pareto-aware sampling which improves the upper or lower performance bounds of the supernet [34]. Predictor can also be used to generate the weights [41] or predict the latency of the network which pushes NAS focusing more on the hardware efficiency [11].

Recently, ranking problem has attracted significant attention. Previous studies adopt the absolute performance, which can be either produced by accuracy predictor or obtained by evaluating, as a metric to guide the following searching procedure. However, the poor ranking correlation between ground-truth performance and evaluated metric of the architectures could deteriorate the searching results [40], since the incorrect predicted rankings caused by the prediction bias will mislead the search algorithm to select the low-ranking architectures. In this case, the predictor based NAS algorithms focus on learning the relative ranking of the neural architectures instead of the absolute ones and can achieve the state-of-the-art results. Re-NAS [4] learns the correct rankings between pairs of architectures by leveraging a ranking loss to punish the disordering predicted metric. CTNAS [37] directly compares two architectures and predicts the probability of one being better than the other. Both of the predictors limit to local

Algorithm 1 NAR Algorithm.

Input: Search space Ω ; encoder and decoder of NAR.

- 1: Randomly draw a set of architectures $\{\alpha^m\}$ from Ω .
- 2: Obtain accuracy y_{α^m} by training α^m
- 3: Build t batches of data, each batch $\{\alpha^m, y_{\alpha^m}\}_{m=1}^k$.
- 4: Initialize five buckets $\{\phi_{T_1}, \dots, \phi_{T_5}\}$ to hold corresponding tier's embedding and statistics, where $\phi_{T_i} = \{\mathbf{e}_{T_i}, \hat{\pi}_{T_i}^{\text{FLOPs}}, \hat{\pi}_{T_i}^{\text{params}}, \hat{\pi}_{T_i}^{\text{operations}}\}$.
- 5: **for** $iter \leftarrow 1 : t$ **do**
- 6: Encode α^m into embedding \mathbf{x}_0^m .
- 7: Build label $\mathbf{l}_i^m = [\mathbb{I}(\alpha^m \in T_1), \dots, \mathbb{I}(\alpha^m \in T_5)]^T$ by equally dividing the batch into five quality tiers with respect to y_{α^m} .
- 8: $\mathbf{x}_{\alpha^m}, \hat{y}_{\alpha^m} = \text{encoder}(\mathbf{x}_0^m)$.
- 9: Compute $\mathcal{L}_1 = \psi(\{\hat{y}_{\alpha^m}\}_{m=1}^k, \{y_{\alpha^m}\}_{m=1}^k)$.
- 10: **for** $i \leftarrow 1 : 5$ **do**
- 11: Get i th tier embedding $\mathbf{e}_i \in \phi_{T_i}$.
- 12: $\mathbf{z}_i = \text{decoder}(\mathbf{e}_i, \mathbf{x}_{\alpha^m})$.
- 13: **end for**
- 14: Sum up $\mathbf{z} = \sum_{i=1}^5 \mathbf{z}_i$ and predict probability \mathbf{p}_{α^m} .
- 15: Compute $\mathcal{L} = \mathcal{L}_2(\mathbf{p}_{\alpha^m}, \mathbf{l}_i^m) + \lambda \mathcal{L}_1$.
- 16: Backward and update parameters of NAR.
- 17: Update tier embeddings and statistics to all buckets.
- 18: **end for**
- 19: **return** Buckets $\{\phi_{T_1}, \dots, \phi_{T_5}\}$; trained NAR.

pair-wise comparison, losing the overall picture of the entire search space. Besides, these comparators which learn a mapping relationship between pair-wise architectures and relative metric, heavily rely on the training data and may not generalize well to unseen architectures.

3. Proposed Method

We propose Neural Architecture Ranker (NAR) to exploit the search space. We first relax the accuracy prediction into a quality classification problem. During the classification, the distributions of the representative parameters of the architectures, e.g., FLOPs, #parameters and node operations, are then collected separately with respect to their quality. Finally, we utilize the distributions of the top tier to guide the sampling procedure, which is free of training an RL controller or employing EA in the searching phase.

3.1. Neural Architecture Ranker

In model design, we utilize the original Transformer [33] to implement the main procedures of *matching and classifying*. Previous work only compares pair-wise architectures and learns a mapping relationship between the extracted features and metric, while we believe the more variety of architectures from the search space the predictor can handle, the more precise and confident the predictor examines

the quality of the architecture. In this way, we first determine five different quality tiers $\mathcal{T} = \{T_1, T_2, T_3, T_4, T_5\}$, according to the ground-truth performance of architectures. For specific architecture α , $\alpha \in T_1$ denotes that the architecture score is among the top 20% rank. Then, we match each sampled architecture with the embedding which represents the population of the networks in each tier, and classify it into the corresponding tier. Algorithm 1 provides the overall meta-algorithm of our Neural Architecture Ranker (NAR). The training pipeline of the NAR is shown in Fig. 1.

Architecture encoding. Similar to ReNAS, we encode each architecture of NAS-Bench-101 and NAS-Bench-201 datasets into feature tensor, $\mathcal{X} \in \mathbb{R}^{N \times P \times P}$, where N denotes the number of the patches and (P, P) is the patch resolution. We put the implementation of encoding in Appendix A. We will release the detailed cell information datasets based on above datasets, including node FLOPs and #parameters in each cell, as well as the feature tensor encoding codes to boost the NAS research one step further.

Once obtain the feature tensor, the \mathcal{X} is reshaped into a sequence of flattened patches $\mathbf{x}_p \in \mathbb{R}^{N \times P^2}$. The \mathbf{x}_p are then mapped to constant dimensions D by a trainable linear projection which is similar to the ViT [10]. We split the tensor into patches in a channel-wise way while ViT is along the image. Position embeddings \mathbf{E}_{pos} which helps keep the architecture macro skeleton information, are added to obtain the input embeddings \mathbf{x}_0 as

$$\mathbf{x}_0 = \mathbf{x}_p \mathbf{E} + \mathbf{E}_{pos}, \quad (4)$$

where $\mathbf{E} \in \mathbb{R}^{P^2 \times D}$ denotes the weights of the linear projection, $\mathbf{E}_{pos} \in \mathbb{R}^{N \times D}$ adopts the original sine and cosine functions for the Transformer.

Supervised architecture feature extraction. We utilize the sampled architecture features for three purposes: 1) compare with the five different tier embeddings and decide which tier it belongs; 2) update the tier embeddings with the classified architecture; 3) predict the relative metric of architecture to guide the selecting procedure in the searching phase. The supervised architecture feature extracting is introduced due to its crucial role in the NAR.

We adopt the encoder to utilize self-attention for extracting needed feature. The encoder stacks $L = 6$ identical layers and each layer consists of a Multiheaded Self-Attention (MSA) block and a fully connected Feed-Forward Network (FFN) block. LayerNorm (LN) is applied to each input of the block, and the block outputs are added with the value passed by the residual connection. We obtain the extracted architecture feature $\mathbf{x}_\alpha \in \mathbb{R}^{N \times D}$ by applying LN to the output feature of the last encoder layer (Eq. (7)).

$$\mathbf{x}'_l = \text{MSA}(\text{LN}(\mathbf{x}_{l-1})) + \mathbf{x}_{l-1}, \quad l = 1, \dots, L, \quad (5)$$

$$\mathbf{x}_l = \text{FFN}(\text{LN}(\mathbf{x}'_l)) + \mathbf{x}'_l, \quad l = 1, \dots, L, \quad (6)$$

$$\mathbf{x}_\alpha = \text{LN}(\mathbf{x}_L). \quad (7)$$

Inspired by the work [4, 40], we employ two layers of linear projection with ReLU activation in-between on the feature \mathbf{x}_α to predict the relative metric \hat{y}_α of the architecture as follows (neglect the bias),

$$\hat{y}_\alpha = \max(0, \mathbf{x}_\alpha \mathbf{W}_r^1) \mathbf{W}_r^2 \quad (8)$$

and adopt the ranking based loss [37] for supervised training

$$\mathcal{L}_1 = \sum_{m=1}^{k-1} \sum_{n=m+1}^k \psi((\hat{y}_{\alpha_m} - \hat{y}_{\alpha_n}) * \text{sign}(y_{\alpha_m} - y_{\alpha_n})), \quad (9)$$

where y_{α_i} is the ground-truth accuracy of architecture α_m , k is the batch size, and $\psi(\epsilon) = \log(1 + e^{-\epsilon})$ denotes the logistic loss function. With the supervised feature extraction, we expect that \mathbf{y}_a is able to prominently distinguish one architecture from others and obtain the correct rankings. This is critical for selecting the best network inside the top tier when sampling described later in Sec. 3.3.

Matching-based tier classification. The decoder is utilized to extract tier embeddings which will be matched in turn with the sampled architecture feature and predict the probabilities of which quality tier it belongs to. The decoder stacks the same number of layers and each layer is inserted by one additional MSA block in addition to the two sub-layers of the encoder.

We initialize five tier embeddings, $\{\mathbf{e}_1, \mathbf{e}_2, \mathbf{e}_3, \mathbf{e}_4, \mathbf{e}_5\}$, where $\mathbf{e}_i \in \mathbb{R}^{N \times D}$. Each tier embedding \mathbf{e}_i represents the architecture information of the corresponding quality tier T_i and is added with the position embeddings, yielding the input \mathbf{z}_i^0 . The first MSA block of the decoder layer acts on \mathbf{z}_i^l and outputs \mathbf{q}_i^l as the Query like the way in Eq. (5). We calculate the cross-attention function by matching the sampled architecture feature \mathbf{x}_α with \mathbf{q}_i^l in the second MSA block as

$$\mathbf{z}_i^l = \text{MSA}(\text{LN}(\mathbf{q}_i^{l-1}), \mathbf{x}_\alpha) + \mathbf{q}_i^{l-1}, \quad l = 1, \dots, L. \quad (10)$$

Then \mathbf{z}_i^l goes through the FFN sub-layer of the decoder as Eq. (6) and in the last stack it yields the output $\mathbf{z}_i = \text{LN}(\mathbf{z}_i^L)$. Notice that we apply above procedure five times to match the architecture with five different tier embeddings. All five outputs are summed up and we apply two layers of learnable linear transformation with ReLU in-between, as well as the softmax function to predict the probabilities of which tier the architecture belongs to:

$$\mathbf{p}_\alpha = \text{softmax}(\max(0, \mathbf{z} \mathbf{W}_p^1) \mathbf{W}_p^2), \quad (11)$$

where $\mathbf{z} = \sum_{i=1}^5 \mathbf{z}_i$ and $\mathbf{p}_\alpha \in \mathbb{R}^5$. We employ cross-entropy loss, denoted as \mathcal{L}_2 , to jointly train the encoder (Eq. (9)) and decoder of the NAR,

$$\mathcal{L} = \mathcal{L}_2 + \lambda \mathcal{L}_1, \quad (12)$$

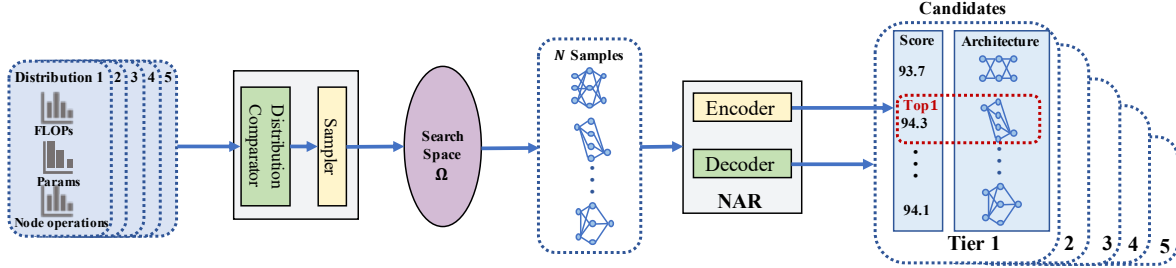


Figure 2. The sampling procedure in the searching phase. First, the distribution of the top tier is used to compare with the ones in the last ranking tiers. Then, the full statistic or only its interval is utilized to sample in the search space. The sampled architectures are ranked and scored by the trained NAR. NAR selects the architecture with highest score in tier 1.

Algorithm 2 Distribution selection.

Input: Tier distributions $\{\hat{\pi}_{T_1}, \dots, \hat{\pi}_{T_5}\}$; batch size k and factor θ ; Kullback-Leibler divergence threshold ζ ; tier index β ($\beta > 1$).

- 1: **for** $i \leftarrow \beta : 5$ **do**
- 2: Compute $d = \text{KL}(\hat{\pi}_{T_1} \parallel \hat{\pi}_{T_i})$.
- 3: **if** #(samples) in $\hat{\pi}_{T_1} < \theta \cdot k$ **or** $d < \zeta$ **then**
- 4: Drop $\hat{\pi}_{T_1}$ possibilities but keep its interval r_{T_1} .
- 5: **return** r_{T_1} .
- 6: **end if**
- 7: **end for**
- 8: **return** $\hat{\pi}_{T_1}$.

where λ controls the importance between two different loss functions. In this way, the NAR manages to extract the feature of the sampled architecture, matching it with the embeddings of all five tiers and deciding its class.

3.2. Tier representation and statistics

Once training one batch of k sampled architectures is completed, their extracted features $\{\mathbf{x}_{\alpha_1}, \mathbf{x}_{\alpha_2}, \dots, \mathbf{x}_{\alpha_k}\}$ obtained by Eq. (7) are updated to corresponding tier embedding \mathbf{e}_i according to their ground-truth tier labels (GT) by calculating the mean value of the features at the end of the iteration t :

$$\mathbf{e}_i^t = \frac{\mathbf{e}_i^{t-1} \sum_{it=1}^{t-1} c_i^{it} + \sum \mathbf{x}_{\alpha_i}}{\sum_{it=1}^t c_i^{it}}, \quad (13)$$

where $\mathbf{x}_{\alpha_i} \in \{\mathbf{x}_\alpha \mid \text{GT}(\alpha) = T_i\}$ and c_i^{it} denote the counts of the architecture features belonging to T_i at iteration it . This is similar to the case when we introduce a memory mechanism to store the features of sampled architectures and leverage them to match with the new ones. Notice that we update according to tier predictions during searching phase since no labels are available during evaluating.

The distributions about FLOPs, #parameters and node operations are also collected to guide the sampling procedure at the same time. For every batch, we discretize the

interval of the FLOPs and #parameters into q constraints equally where size is calculated as

$$\delta' = \frac{\tau_{\max} - \tau_{\min}}{q}, \quad (14)$$

where τ_{\max} and τ_{\min} are the maximum and minimum of the FLOPs or #parameters, respectively, in one batch. We round up the step $\delta = \lceil \delta' \rceil$ and then empirically approximate the distributions $\pi(\tau)$ as follows,

$$\hat{\pi}(\tau_\kappa) = \frac{\#(\tau_\kappa = \tau_{\min} + \kappa \cdot \delta)}{k}, \quad \kappa = 1, \dots, q \quad (15)$$

where τ_κ denotes the κ th constraints on the interval, $\#(\tau_\kappa)$ denotes the number of the architecture located in constraint range $(\tau_{\kappa-1}, \tau_\kappa]$ for FLOPS or #parameters. As for every type of node operation, we just collect its total counts in each tier without discretization. Different from the offline way in AttentiveNAS [34], we train the NAR and simultaneously count the distributions for different quality tiers, $\{\hat{\pi}_{T_i}(\tau_\kappa) \mid i = 1, \dots, 5; \kappa = 1, \dots, q\}$. In this way, we have a thorough understanding about the hierarchical distribution of the search space for guiding the sampling process.

3.3. Searching with tier statistics

We utilize the trained NAR and the collected distributions to guide the searching phase. Distributions of FLOPs, #parameters and node operations are carefully selected first. Because, for some cases, one distribution depicting the top tier may be similar to those of low ranking tiers. Therefore, we apply Kullback-Leibler divergence to measure the difference between top and last ranking distributions as shown in Algorithm 2. Specifically, once the divergence is less than the specified threshold, we discard the possibilities of distribution but sample architectures randomly on the interval. Noted that, this is not equivalent to discarding the entire distribution since we still sample on the interval where good candidates may locate in. Besides, we sample randomly on the interval in the same way when the population of the top tier is less than specific proportion of the sample size.

Table 1. Search results on the NAS-Bench-101 search space. ‘‘Average Accuracy’’ denotes the average of the classification accuracy (%) of the best architecture searched in each run on CIFAR-10 dataset. ‘‘Best Accuracy’’ and ‘‘Best Rank’’ denote the classification accuracy (%) and thousandth rank of the best architecture searched in all runs. ‘‘†’’ denotes our implementation. All experiments are run 10 times.

Methods	Average Accuracy (%)	Best Accuracy (%)	Best Rank (%)	Cost (seconds)	
				train	search
DARTS [21]	92.21±0.61	93.02	13.47	-	-
ENAS [26]	91.83±0.42	92.54	22.88	-	-
FairNAS [6]	91.10±1.84	93.55	0.77	-	-
SPOS [13]	89.85±3.80	93.84	0.07	-	-
FBNet [36]	92.29±1.25	93.98	0.05	-	-
CTNAS† [4]	93.91±0.13	94.14	0.02	188.37	750.97
ReNAS† [37]	93.96±0.08	94.02	0.09	73.68	-
NAR (random)	94.04±0.07	94.11	0.03	255.86	53.51
NAR (statistics)	94.05±0.09	94.19	0.01	292.61	189.94

For every iteration, we sample k subnets from the search space. Specifically we sample FLOPs and #parameters as constraints with the selected distributions yielded in Algorithm 2 and reuse the constraints for every m ($m < k$) subnets. The implementation of the architectures sampling for NAS-Bench-101 and NAS-Bench-201 are detailed in Appendix B. After sampling the architecture, we build the subnet and reject those exceeding the constraints. In addition, we randomly sample certain proportion of subnets from the entire search space to increase the diversity.

Giving a batch of k samples, we leverage the trained NAR to rank and score the architectures, *i.e.*, select top 5 architectures according to the predicted score in the classified tier T_1 as candidates at each iteration. Then, We train these candidates and obtain their evaluated accuracy. Thus, our sampling method fully exploits the knowledge of the training set to approximate the search space and achieves a top quality aware sampling procedure. The sampling procedure in the searching phase is shown in Fig. 2.

4. Experiments

In this section, we have verify the effectiveness of the proposed NAR and sampling method on two widely accepted NAS search space, namely NAS-Bench-101 [38] and NAS-Bench-201 [9]. All our experiments are implemented on a single NVIDIA TITAN RTX GPU. The learning rate schedule and positional embeddings closely follow the settings from the Transformer [33]. We adopt AdamW [23] as the optimizer in our experiments. The NAR codes and the detailed cell information datasets will be released at <https://github.com/AlbertiPot/nar.git>.

4.1. Architecture search results on NAS-Bench-101

We verify the effectives of the proposed NAR method on the NAS-Bench-101 dataset, which is a cell-based dataset

containing over 423k unique convolutional architectures. All of the architectures are trained on the CIFAR-10 for 3 times to obtain the validation and test accuracy. We randomly sample 1% (4236) of the architectures and their averaged accuracy as our training set and another 1024 architectures as the validation set. Two types of sampling methods are tested: 1) *random*: randomly sample one batch of architectures from the entire search space in every iteration; 2) *statistics*: randomly sample a certain proportion of architectures and the rest of the batch are sampled with the collected distributions of FLOPs and #parameters. The detailed training settings are listed in Appendix C.

The proposed method is compared with the state-of-the-art NAS method and main results are shown in Tab. 1. All of the experiments are repeated 10 times with different random seeds. For fair comparison, we re-implement the recent state-of-the-art work [4, 37] with the same random seeds and the training set size. As shown in Tab. 1, the proposed NAR combined with *random* or *statistics* sampling method achieves new state-of-the-art performance. With *statistics* sampling, the proposed NAR framework outperforms other competitors on the average accuracy with relative low variance. Even more, it finds the individual architecture with top 0.01% performance among the search space. The fact of achieving the superior performance is attributed to three reasons: 1) the NAR is capable of well classifying the architectures of all tiers from the search space; 2) the combination of the use of the collected distributions and the random sampling method; 3) the adopted ranking based loss is helpful to score the top architectures correctly. With *random sampling*, the proposed NAR performs slightly worse than *statistics* but still works better and more stable than the competitors. This demonstrates the superiority of the NAR for distinguishing top architectures given a random candidates. Without the collected distributions, it finds the individual architecture with top 0.03% performance among the

Table 2. Search results on the NAS-Bench-201 search space. ‘‘validation’’ and ‘‘test’’ denote the classification accuracy (%) on the validation set and test set, respectively. ‘‘average’’ denotes the average of the classification accuracy (%) of the best architecture searched in each run; ‘‘best’’ denotes the classification accuracy (%) of the best architecture searched in all runs. ‘‘Optimal’’ denotes the highest accuracy for each set. In the searching phase, only the interval of the collected distribution is adopted to sample architectures. The cost of the NAR framework reported includes the total cost of training and searching. All our experiments are run 10 times.

Methods	Cost (seconds)	CIFAR-10		CIFAR-100		ImageNet-16-120	
		validation	test	validation	test	validation	test
RSPS [17]	7587	87.60±0.61	91.05±0.66	68.27±0.72	68.26±0.96	39.73±0.34	40.69±0.36
SETN [8]	31010	90.00±0.97	92.72±0.73	69.19±1.42	69.36±1.72	39.77±0.33	39.51±0.33
ENAS [26]	13315	90.20±0.00	93.76±0.00	70.21±0.71	70.67±0.62	40.78±0.00	41.44±0.00
FairNAS [6]	9845	90.07±0.57	93.23±0.18	70.94±0.94	71.00±1.46	41.90±1.00	42.19±0.31
ReNAS [37]	86.31	90.90±0.31	93.99±0.25	71.96±0.99	72.12±0.79	45.85±0.47	45.97±0.49
GenNAS [18]	1080	-	94.18±0.10	-	72.56±0.74	-	45.59±0.54
DARTS- [5]	11520	91.03±0.44	93.80±0.40	71.36±1.51	71.53±1.51	44.87±1.46	45.12±0.82
BOHB [12]	3.59	91.17±0.27	93.94±0.28	72.04±0.93	72.00±0.86	45.55±0.79	45.70±0.86
NAR (average)	168.99	91.44±0.10	94.33±0.05	72.54±0.44	72.89±0.37	46.16±0.37	46.66±0.23
NAR (best)	168.99	91.61	94.37	73.49	73.51	46.50	47.31
Optimal	-	91.61	94.37	73.49	73.51	46.73	47.31

search space, which is still competitive to others.

As for search cost, the proposed sampling methods cost lower compared to the CTNAS in which a LSTM is trained to generate architectures during searching. When sampling with *random*, it achieves the lowest cost since it does not require rejection sampling. Different from encoding the architectures beforehand in ReNAS, our pipeline encodes architectures and trains the NAR simultaneously which costs more but is closer to the real application. ReNAS achieves the lowest training cost because it adopts LeNet-5 as the predictor while we utilize the advanced Transformer.

4.2. Architecture search results on NAS-Bench-201

NAS-Bench-201 is also a cell-based dataset with 15625 unique convolutional architectures and corresponding training, validation and test accuracy trained on CIFAR-10, CIFAR-100 and ImageNet-16-120 datasets. We randomly sample 1000 architectures with their validation accuracy from the entire search space as our training set, and another 256 architectures as the validation set. The training and searching are the same with NAS-Bench-101 except for we sample randomly on the interval of the collected distribution since the search space is small. We compare the performance of the NAR with other NAS methods in Tab. 2. The proposed NAR achieves new state-of-the-art average validation and test accuracy on all of three datasets with relative low variance. It demonstrates that our NAR is capable of finding the top quality architectures more stably compared to the competitors. Besides, adequate training samples which can offer useful distribution under acceptable evaluation cost are key to the good performance. Fur-

Table 3. Comparisons of different proportions (p) of randomly sampled architectures. All experiments under different p are run 10 times on the NAS-Bench-101 dataset.

p	Average Acc. (%)	Best Acc. (%)
0.0	93.92±0.12	94.22
0.3	93.98±0.08	94.17
0.5	94.05±0.09	94.19
0.7	94.04±0.05	94.14
1.0	94.04±0.07	94.11

thermore, the proposed method finds the optimal architecture which holds highest test classification accuracy among 3 datasets, proving the superiority and generality of the proposed NAR framework. The total cost consists of training at 126 seconds and searching cost at 51 seconds, which are both acceptable and competitive.

5. Ablation Study

5.1. Effect of random samples

In order to investigate the effect of the proportion of the randomly sampled architectures, we conduct more experiments on the NAS-Bench-101 search space. As shown in Tab. 3, when sampling entirely with the distribution collected during training ($p = 0$), the NAR framework finds the superior individual architecture but with a relative lower and more unstable average accuracy. However, with a certain proportion of randomly sampled architectures $p \in 0.3, 0.5, 0.7$ added in or even all ($p = 1$), the proposed

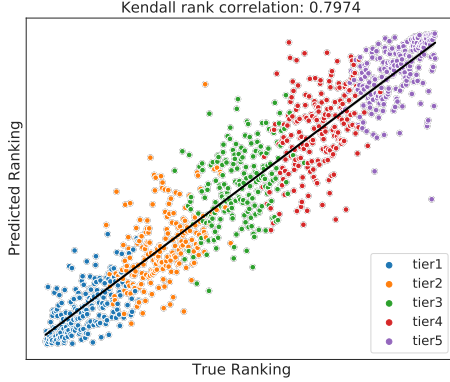


Figure 3. Rank correlation between the predicted ranking and the actual ranking of the proposed NAR. 1024 architectures are randomly sampled from the NAS-Bench-101 dataset. Architectures are marked with their ground-truth tier. Kendall’s $\tau = 0.7974$ is obtained in one trial of ten experiments.

Table 4. Comparisons of the proposed NAR trained with and without ranking based loss. All experiments are run 10 times on the NAS-Bench-101 dataset.

Ranking loss	Average Acc. (%)	Kendall’s τ
✗	93.99 ± 0.09	-
✓	94.05 ± 0.09	0.7971

method reaches a high mean accuracy. This may attribute to two points: 1) the distribution is collected in each batch during the training, and distributions from all batches will be used by turns across all sampling iterations, so the samples of each distribution might not be adequate; 2) The NAR is trained with different tiers of architectures while it can not compare and distinguish architectures from the same tier, so we propose to add certain proportion of randomly sampled architectures to the batch to improve the data diversity.

One more thing, the accuracy of the best found architectures are higher when sample with low random proportion. This demonstrates that the collected distributions does help to sample good candidates in large search space.

5.2. Effect of the ranking based loss

To verify the effectiveness of the ranking based loss, we compare the results of our NAR ($p = 0.5$) trained with and without the ranking loss. For the latter, the architectures with top 5 predicted classification probabilities p_α from tier T_1 are selected as candidates. As shown in Tab. 4, the NAR trained only with cross-entropy loss achieves competitive results compared to previous methods in Tab. 1 and with the help of the ranking loss, the NAR achieves slightly better. This demonstrates the NAR is capable of distinguishing individual architectures of good quality and we strength it by

Table 5. Comparisons of different number of the selected architectures during search phase. “top- k ” denotes the k architectures with the highest prediction scores. “Queries” denotes the total number of queries to the ground-truth test accuracy for 50 iterations. All experiments are run 10 times on the NAS-Bench-101 dataset.

top- k	Average Acc. (%)	Queries	Ranking loss
1	94.02 ± 0.11	50	✓
3	94.04 ± 0.09	150	
5	94.05 ± 0.09	250	
7	94.05 ± 0.08	350	
10	94.05 ± 0.08	500	
1	93.82 ± 0.08	50	✗
5	93.99 ± 0.09	250	✗

further improving the ranking ability. The average ranking correlation (Kendall’s τ) between the predicted and actual accuracy is 0.7971 on the validation set. We further visualize the ranking and tier classification results in Fig. 3.

5.3. Evaluate cost in sampling procedure

During the search phase, we sample for 50 iterations and select the top 5 architectures to query their test accuracies in every iteration, which are total 250 architectures to evaluate. In other words, the less architectures selected, the more evaluate cost we save. This requires the NAR holds high ranking and classification ability to ensure that we can find the outperforming candidates under limit selection trials. We compare the results of different number of the selected architectures in Tab. 5. It shows that the NAR can still achieve higher performance even with only one architecture selected, which dramatically reduces the search cost. We further investigate the results of the NAR trained without ranking loss, the average accuracy degrades more when one architecture selected. This demonstrates the ranking based loss is essential to improve the ranking ability.

6. Conclusion

In this work, we propose the Neural Architecture Ranker to rank and score the architectures for improving the searching efficiency of NAS. The NAR framework classifies the architectures into five different quality tiers and scores them with the relative metric. The tier distributions are collected to guide the sampling during the searching phase which is free of excessive searching cost. Our methods outperforms previous NAS competitors on both the NAS-Bench-101 and NAS-Bench-201 datasets, stably finding the superior architectures from the search space with competitive cost. We will release two detailed cell information datasets to boost in-depth research into the micro structure in NAS field.

References

[1] Han Cai, Chuang Gan, Tianzhe Wang, Zhekai Zhang, and Song Han. Once-for-all: Train one network and specialize it for efficient deployment. In *International Conference on Learning Representations*, 2020. 1, 3

[2] Han Cai, Ligeng Zhu, and Song Han. ProxylessNAS: Direct neural architecture search on target task and hardware. In *International Conference on Learning Representations*, 2019. 1

[3] Liang-Chieh Chen, George Papandreou, Iasonas Kokkinos, Kevin Murphy, and Alan L. Yuille. Semantic image segmentation with deep convolutional nets and fully connected crfs. In Yoshua Bengio and Yann LeCun, editors, *3rd International Conference on Learning Representations, ICLR 2015, San Diego, CA, USA, May 7-9, 2015, Conference Track Proceedings*, 2015. 1

[4] Yaofu Chen, Yong Guo, Qi Chen, Minli Li, Wei Zeng, Yaowei Wang, and Mingkui Tan. Contrastive neural architecture search with neural architecture comparators. In *Proceedings of the IEEE/CVF Conference on Computer Vision and Pattern Recognition (CVPR)*, pages 9502–9511, June 2021. 1, 3, 4, 6

[5] Xiangxiang Chu, Xiaoxing Wang, Bo Zhang, Shun Lu, Xiaolin Wei, and Junchi Yan. {DARTS}-: Robustly stepping out of performance collapse without indicators. In *International Conference on Learning Representations*, 2021. 7

[6] Xiangxiang Chu, Bo Zhang, and Ruijun Xu. Fairnas: Rethinking evaluation fairness of weight sharing neural architecture search. In *Proceedings of the IEEE/CVF International Conference on Computer Vision (ICCV)*, pages 12239–12248, October 2021. 2, 6, 7

[7] Xiaoliang Dai, Alvin Wan, Peizhao Zhang, Bichen Wu, Zijian He, Zhen Wei, Kan Chen, Yuandong Tian, Matthew Yu, Peter Vajda, and Joseph E. Gonzalez. Fbnetsv3: Joint architecture-recipe search using predictor pretraining. In *Proceedings of the IEEE/CVF Conference on Computer Vision and Pattern Recognition (CVPR)*, pages 16276–16285, June 2021. 3

[8] Xuanyi Dong and Yi Yang. One-shot neural architecture search via self-evaluated template network. In *Proceedings of the IEEE/CVF International Conference on Computer Vision (ICCV)*, October 2019. 7

[9] Xuanyi Dong and Yi Yang. Nas-bench-201: Extending the scope of reproducible neural architecture search. In *International Conference on Learning Representations*, 2020. 6

[10] Alexey Dosovitskiy, Lucas Beyer, Alexander Kolesnikov, Dirk Weissenborn, Xiaohua Zhai, Thomas Unterthiner, Mostafa Dehghani, Matthias Minderer, Georg Heigold, Sylvain Gelly, Jakob Uszkoreit, and Neil Houlsby. An image is worth 16x16 words: Transformers for image recognition at scale. In *International Conference on Learning Representations*, 2021. 4

[11] Lukasz Dudziak, Thomas Chau, Mohamed Abdelfattah, Roysen Lee, Hyeji Kim, and Nicholas Lane. Brp-nas: Prediction-based nas using gcns. In H. Larochelle, M. Ranzato, R. Hadsell, M. F. Balcan, and H. Lin, editors, *Advances in Neural Information Processing Systems*, volume 33, pages 10480–10490. Curran Associates, Inc., 2020. 3

[12] Stefan Falkner, Aaron Klein, and Frank Hutter. BOHB: Robust and efficient hyperparameter optimization at scale. In Jennifer Dy and Andreas Krause, editors, *Proceedings of the 35th International Conference on Machine Learning*, volume 80 of *Proceedings of Machine Learning Research*, pages 1437–1446. PMLR, 10–15 Jul 2018. 7

[13] Zichao Guo, Xiangyu Zhang, Haoyuan Mu, Wen Heng, Zechun Liu, Yichen Wei, and Jian Sun. Single path one-shot neural architecture search with uniform sampling. In Andrea Vedaldi, Horst Bischof, Thomas Brox, and Jan-Michael Frahm, editors, *Computer Vision – ECCV 2020*, pages 544–560, Cham, 2020. Springer International Publishing. 2, 6

[14] Irtiza Hasan, Shengcai Liao, Jinpeng Li, Saad Ullah Akram, and Ling Shao. Generalizable pedestrian detection: The elephant in the room. In *Proceedings of the IEEE/CVF Conference on Computer Vision and Pattern Recognition (CVPR)*, pages 11328–11337, June 2021. 1

[15] Kaiming He, Xiangyu Zhang, Shaoqing Ren, and Jian Sun. Deep residual learning for image recognition. In *Proceedings of the IEEE Conference on Computer Vision and Pattern Recognition (CVPR)*, June 2016. 1

[16] Andrew Howard, Mark Sandler, Grace Chu, Liang-Chieh Chen, Bo Chen, Mingxing Tan, Weijun Wang, Yukun Zhu, Ruoming Pang, Vijay Vasudevan, Quoc V. Le, and Hartwig Adam. Searching for mobilenetv3. In *Proceedings of the IEEE/CVF International Conference on Computer Vision (ICCV)*, October 2019. 2

[17] Liam Li and Ameet Talwalkar. Random search and reproducibility for neural architecture search. In Ryan P. Adams and Vibhav Gogate, editors, *Proceedings of The 35th Uncertainty in Artificial Intelligence Conference*, volume 115 of *Proceedings of Machine Learning Research*, pages 367–377. PMLR, 22–25 Jul 2020. 7

[18] Yuhong Li, Cong Hao, Pan Li, Jinjun Xiong, and Deming Chen. Generic neural architecture search via regression. *CoRR*, abs/2108.01899, 2021. 7

[19] Chenxi Liu, Barret Zoph, Maxim Neumann, Jonathon Shlens, Wei Hua, Li-Jia Li, Li Fei-Fei, Alan Yuille, Jonathan Huang, and Kevin Murphy. Progressive neural architecture search. In *Proceedings of the European Conference on Computer Vision (ECCV)*, September 2018. 3

[20] Hanxiao Liu, Karen Simonyan, Oriol Vinyals, Chrisantha Fernando, and Koray Kavukcuoglu. Hierarchical representations for efficient architecture search. In *International Conference on Learning Representations*, 2018. 1, 2

[21] Hanxiao Liu, Karen Simonyan, and Yiming Yang. DARTS: Differentiable architecture search. In *International Conference on Learning Representations*, 2019. 1, 6

[22] Jonathan Long, Evan Shelhamer, and Trevor Darrell. Fully convolutional networks for semantic segmentation. In *Proceedings of the IEEE Conference on Computer Vision and Pattern Recognition (CVPR)*, June 2015. 1

[23] Ilya Loshchilov and Frank Hutter. Decoupled weight decay regularization. In *International Conference on Learning Representations*, 2019. 6

[24] Zhichao Lu, Gautam Sreekumar, Erik Goodman, Wolfgang Banzhaf, Kalyanmoy Deb, and Vishnu Naresh Boddeti. Neural architecture transfer. *IEEE Transactions on Pattern Analysis and Machine Intelligence*, 43(9):2971–2989, 2021. 2

[25] Renqian Luo, Fei Tian, Tao Qin, Enhong Chen, and Tie-Yan Liu. Neural architecture optimization. In S. Bengio, H. Wallach, H. Larochelle, K. Grauman, N. Cesa-Bianchi, and R. Garnett, editors, *Advances in Neural Information Processing Systems*, volume 31. Curran Associates, Inc., 2018. 1

[26] Hieu Pham, Melody Guan, Barret Zoph, Quoc Le, and Jeff Dean. Efficient neural architecture search via parameters sharing. In Jennifer Dy and Andreas Krause, editors, *Proceedings of the 35th International Conference on Machine Learning*, volume 80 of *Proceedings of Machine Learning Research*, pages 4095–4104. PMLR, 10–15 Jul 2018. 1, 2, 6, 7

[27] Esteban Real, Alok Aggarwal, Yanping Huang, and Quoc V. Le. Regularized evolution for image classifier architecture search. *Proceedings of the AAAI Conference on Artificial Intelligence*, 33(01):4780–4789, Jul. 2019. 1, 2

[28] Esteban Real, Sherry Moore, Andrew Selle, Saurabh Saxena, Yutaka Leon Suematsu, Jie Tan, Quoc V. Le, and Alexey Kurakin. Large-scale evolution of image classifiers. In Doina Precup and Yee Whye Teh, editors, *Proceedings of the 34th International Conference on Machine Learning*, volume 70 of *Proceedings of Machine Learning Research*, pages 2902–2911. PMLR, 06–11 Aug 2017. 2

[29] Joseph Redmon, Santosh Divvala, Ross Girshick, and Ali Farhadi. You only look once: Unified, real-time object detection. In *Proceedings of the IEEE Conference on Computer Vision and Pattern Recognition (CVPR)*, June 2016. 1

[30] Shaoqing Ren, Kaiming He, Ross Girshick, and Jian Sun. Faster r-cnn: Towards real-time object detection with region proposal networks. In C. Cortes, N. Lawrence, D. Lee, M. Sugiyama, and R. Garnett, editors, *Advances in Neural Information Processing Systems*, volume 28. Curran Associates, Inc., 2015. 1

[31] Karen Simonyan and Andrew Zisserman. Very deep convolutional networks for large-scale image recognition. In Yoshua Bengio and Yann LeCun, editors, *3rd International Conference on Learning Representations, ICLR 2015, San Diego, CA, USA, May 7-9, 2015, Conference Track Proceedings*, 2015. 1

[32] Mingxing Tan, Bo Chen, Ruoming Pang, Vijay Vasudevan, Mark Sandler, Andrew Howard, and Quoc V. Le. Mnasnet: Platform-aware neural architecture search for mobile. In *Proceedings of the IEEE/CVF Conference on Computer Vision and Pattern Recognition (CVPR)*, June 2019. 2

[33] Ashish Vaswani, Noam Shazeer, Niki Parmar, Jakob Uszkoreit, Llion Jones, Aidan N Gomez, Łukasz Kaiser, and Illia Polosukhin. Attention is all you need. In I. Guyon, U. V. Luxburg, S. Bengio, H. Wallach, R. Fergus, S. Vishwanathan, and R. Garnett, editors, *Advances in Neural Information Processing Systems*, volume 30. Curran Associates, Inc., 2017. 3, 6

[34] Dilin Wang, Meng Li, Chengyue Gong, and Vikas Chandra. Attentivenas: Improving neural architecture search via attentive sampling. In *Proceedings of the IEEE/CVF Conference on Computer Vision and Pattern Recognition (CVPR)*, pages 6418–6427, June 2021. 3, 5

[35] Wei Wen, Hanxiao Liu, Yiran Chen, Hai Li, Gabriel Bender, and Pieter-Jan Kindermans. Neural predictor for neural architecture search. In Andrea Vedaldi, Horst Bischof, Thomas Brox, and Jan-Michael Frahm, editors, *Computer Vision – ECCV 2020*, pages 660–676, Cham, 2020. Springer International Publishing. 1

[36] Bichen Wu, Xiaoliang Dai, Peizhao Zhang, Yanghan Wang, Fei Sun, Yiming Wu, Yuandong Tian, Peter Vajda, Yangqing Jia, and Kurt Keutzer. Fbnet: Hardware-aware efficient convnet design via differentiable neural architecture search. In *Proceedings of the IEEE/CVF Conference on Computer Vision and Pattern Recognition (CVPR)*, June 2019. 6

[37] Yixing Xu, Yunhe Wang, Kai Han, Yehui Tang, Shangling Jui, Chunjing Xu, and Chang Xu. Renas: Relativistic evaluation of neural architecture search. In *Proceedings of the IEEE/CVF Conference on Computer Vision and Pattern Recognition (CVPR)*, pages 4411–4420, June 2021. 1, 3, 4, 6, 7, 11

[38] Chris Ying, Aaron Klein, Eric Christiansen, Esteban Real, Kevin Murphy, and Frank Hutter. NAS-bench-101: Towards reproducible neural architecture search. In Kamalika Chaudhuri and Ruslan Salakhutdinov, editors, *Proceedings of the 36th International Conference on Machine Learning*, volume 97 of *Proceedings of Machine Learning Research*, pages 7105–7114. PMLR, 09–15 Jun 2019. 1, 6

[39] Jiahui Yu, Pengchong Jin, Hanxiao Liu, Gabriel Bender, Pieter-Jan Kindermans, Mingxing Tan, Thomas Huang, Xiaodan Song, Ruoming Pang, and Quoc Le. Bignas: Scaling up neural architecture search with big single-stage models. In Andrea Vedaldi, Horst Bischof, Thomas Brox, and Jan-Michael Frahm, editors, *Computer Vision – ECCV 2020*, pages 702–717, Cham, 2020. Springer International Publishing. 3

[40] Kaicheng Yu, Rene Ranftl, and Mathieu Salzmann. Landmark regularization: Ranking guided super-net training in neural architecture search. In *Proceedings of the IEEE/CVF Conference on Computer Vision and Pattern Recognition (CVPR)*, pages 13723–13732, June 2021. 3, 4

[41] Chris Zhang, Mengye Ren, and Raquel Urtasun. Graph hypernetworks for neural architecture search. In *International Conference on Learning Representations*, 2019. 3

[42] Yunpeng Zhang, Jiwen Lu, and Jie Zhou. Objects are different: Flexible monocular 3d object detection. In *Proceedings of the IEEE/CVF Conference on Computer Vision and Pattern Recognition (CVPR)*, pages 3289–3298, June 2021. 1

[43] Yifu Zhang, Chunyu Wang, Xinggang Wang, Wenjun Zeng, and Wenyu Liu. Fairmot: On the fairness of detection and re-identification in multiple object tracking. *International Journal of Computer Vision*, 129(11):3069–3087, Sep 2021. 1

[44] Barret Zoph and Quoc V. Le. Neural architecture search with reinforcement learning. In *5th International Conference on Learning Representations, ICLR 2017, Toulon, France, April 24–26, 2017, Conference Track Proceedings*, 2017. 2

A. Architecture representation

For NAS-Bench-101, each cell of the network contains at most 7 nodes, and there are total 9 cells. Nodes in each cell are denoted as operations and edges as connections. Following ReNAS [37], cell connection is modeled by an adjacent matrix $\mathcal{A} \in \{0, 1\}^{7 \times 7}$. When nodes are less than 7, we pad the missing rows and columns with 0. An operation type vector $\mathbf{o} \in \{1, \dots, 5\}^5$ is built to represent IN node, 1×1 convolution, 3×3 convolution, 3×3 max-pooling and OUT node, respectively. Besides, in order to represent the computational ability of the cell, the FLOPs and #parameters of each node are calculated, and formed into FLOP vector $\mathbf{f} \in \mathbb{R}^7$ and #parameters vector $\mathbf{p} \in \mathbb{R}^7$ for all nodes in each cell, where the missing nodes are padded with 0 when nodes of the cell are less than 7. Vectors \mathbf{o} is first broadcast into matrices, and then element-wisely multiplied with the adjacent matrix \mathcal{A} to form the operation matrix \mathbf{O} . Vectors \mathbf{f} and \mathbf{p} of each cell are transformed into the FLOPs matrix \mathbf{F} and #parameters matrix \mathbf{P} in the same way. Finally, operation matrix \mathbf{O} and matrices of all cells are concatenated into one feature tensor \mathcal{X} , whose size is $(19, 7, 7)$.

For NAS-Bench-201, each node represents the sum of the feature maps and each edge as an operation. Every architecture has fixed 4 nodes and we build an adjacent matrix $\mathcal{A} \in \{0, 1\}^{4 \times 4}$ without padding. The operation vector $\mathbf{o} \in \{0, \dots, 4\}^5$ represents zeroize, skip connect, 1×1 convolution, 3×3 convolution and 3×3 avg-pooling. The FLOPs vector $\mathbf{f} \in \mathbb{R}^4$ and the #parameters vector $\mathbf{p} \in \mathbb{R}^4$ are obtained identically and broadcast into matrices. We concatenate those matrices according to the order of the cells and obtain the final feature tensor \mathcal{X} with size $(31, 4, 4)$. Every two matrices, from the second matrix to the last, correspond to the FLOPs and #parameters of nodes for each cell, except for the first matrix representing the operations.

B. Sampling details

The sample size is the same as the training batch size. As discussed in Sec. 5.1, we set $p = 0.5$ to balance between the stable average accuracy and the superior individual selection ability. The constraints are reused for every 25 sampling trials and we sample total 50 iterations. For variables in Algorithm 2, thresholds ζ of Kullback-Leibler divergence for FLOPs and #parameters are both 2.5, the batch factor $\theta = 0.1$ and tier index $\beta = 4$.

For total 7 nodes of the cell in NAS-Bench-101, traversing from the second node (the first node is IN node) to the last OUT node, we first randomly sample from previous nodes of one specific node to build the connection, then sample the operation type of the node according to the distribution collected during training. For the remaining 3 edges (maximum 9 edges in each cell), two nodes are randomly sampled to build the connection and we repeat the

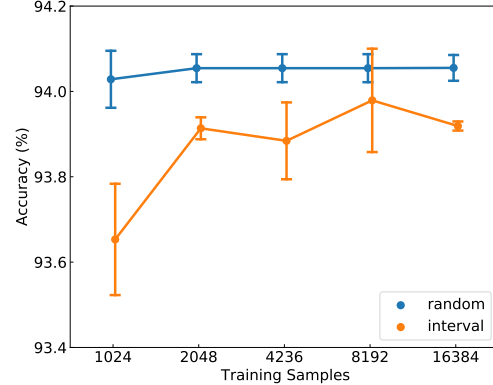


Figure 4. The effect of different number of training samples. “random” denotes that architectures are randomly sampled from the search space; “interval” denotes that architectures are randomly sampled on the interval of the distribution. All experiments are run 5 times on the NAS-Bench-101 dataset.

procedure for 3 times. For NAS-Bench-201, since each cell has 4 nodes with fixed connection (each node connects to all of its previous nodes), we only sample the operation type for the edges of all nodes.

C. Training settings

For NAS-Bench-101, the AdamW optimizer is set with $\beta_1 = 0.9$, $\beta_2 = 0.982$, weight decay term is 5×10^{-4} and $\epsilon = 10^{-9}$. The batch size is set to 256 and the NAR is trained for 35 epochs with 50 iterations as warm-up. For NAS-Bench-201, the AdamW optimizer is set with $\beta_1 = 0.9$, $\beta_2 = 0.99$, weight decay term is 1×10^{-2} and $\epsilon = 10^{-9}$. The batch size is set to 128 and the NAR is trained for 55 epochs with 30 iterations as warm-up.

D. The number of training samples

The training samples are not only used to train the NAR, but also utilized to collect the distributions of all tiers. We further investigate the effect of the number of the training samples, *i.e.*, train and collect on $\{1024, 2048, 4236, 8192, 16384\}$ architectures randomly sampled from the NAS-Bench-101 dataset. Since the training size could affect the selection of the Kullback-Leibler divergence thresholds when sampling, we perform two kinds of random sampling during the searching phase: 1) randomly sample from the entire search space, denoted as *random*; 2) randomly sample a batch of architectures on the interval of the collected distribution in every iteration, denoted as *interval*. As shown in Fig. 4, when the samples size is 1024, the accuracy deteriorates significantly. Moreover, random sampling performs better and more stably over sampling on the interval. This requires that we add certain proportion of randomly sampled architectures as discussed in Sec. 5.1.